J|A|C|S
ARTICLES
Published on Web 06/19/2007

Toward Controlled Spacing in One-Dimensional Molecular Chains: Alkyl-Chain-Functionalized Fullerenes in Carbon Nanotubes

Thomas W. Chamberlain,[†] Andrew Camenisch,[†] Neil R. Champness,[†] G. Andrew D. Briggs,[‡] Simon C. Benjamin,[‡] Arzhang Ardavan,[§] and Andrei N. Khlobystov*,[†]

Contribution from the School of Chemistry, University of Nottingham, Nottingham NG7 2RD, United Kingdom, Department of Materials, University of Oxford, Oxford OX1 3PH, United Kingdom, and Department of Physics, University of Oxford, Oxford OX1 3PU, United Kingdom

Received March 14, 2007; E-mail: Andrei.Khlobystov@nottingham.ac.uk

Abstract: A range of fullerenes (C_{60}) functionalized with long alkyl chains have been synthesized and inserted into single-walled carbon nanotubes. The impact of the alkyl chain length and of the type of linker between the addend and the fullerene cage on the geometry of molecular arrays in nanotube has been studied by high-resolution transmission electron microscopy. In the presence of functional groups the mean interfullerene separations are significantly increased by 2−8 nm depending on the length of the alkyl chain, but the periodicity of the fullerene arrays is disrupted due to the conformational flexibility of the alkyl groups.

Introduction

Due to their tubular nature, carbon nanotubes have been demonstrated to encapsulate different molecules, thus forming quasi-one-dimensional molecular systems.[1,2] For example, fullerenes can be inserted in single-walled carbon nanotubes (SWNTs) to form encapsulated, linear chains of molecules termed peapods (Figure 1).[3] These structures give a unique opportunity to study the physicochemical properties of the molecular species confined in a nanosized container. It has been demonstrated that, for example, molecular motion (translational and rotational), molecular orientation, packing, and chemical reactivity are substantially affected by confinement in nanotubes,[4−8] with the nanotube diameter being the most important geometric parameter controlling the structures and properties of encapsulated molecular arrays.

As a result of encapsulation in nanotubes, intermolecular interactions between fullerenes are expected to be altered substantially compared with the bulk crystal. The energy gained when a fullerene enters a nanotube is manifested as a 0.5 nN force on each C_{60},[9] driving the fullerene into the nanotube. On the basis of this observation, it has also been suggested that an effective pressure of about 1 GPa exists inside a fullerene-filled nanotube.[10] However, the diffraction measurements and high-resolution transmission electron microscopy (HRTEM) studies show that the interfullerene distance in SWNT for C_{60} almost invariably falls in the range 9.7−10.0 Å,[11−14] which is very close to the interfullerene separation in the bulk face-centered cubic (fcc) crystal (10.04 Å).[15] Larger fullerenes C_{70}−C_{92} and their endohedral derivatives were shown to have slightly longer separations, typically between 10.1 and 11.4 Å,[11,16−19] which

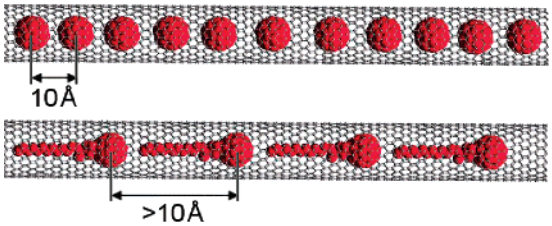

Figure 1. Structure of a peapod system (top) and the proposed method of increasing the interfullerene separation of peapod systems by use of a fullerene functionalized with a long alkyl chain (bottom).

[†] University of Nottingham.
[‡] Department of Materials, University of Oxford.
[§] Department of Physics, University of Oxford.

(1) Monthioux, M. *Carbon* **2002**, *40*, 1809−1822 and references therein.
(2) Smith, B. W.; Monthioux, M.; Luzzi, E. D. *Nature* **1998**, *396*, 323−324.
(3) Khlobystov, A. N.; Britz, D. A.; Wang, J.; O'Neil, S. A.; Poliakoff, M.; Briggs, G. A. D. *J. Mater. Chem.* **2004**, *14*, 2852−2857.
(4) Khlobystov, A. N.; Britz, D. A.; Briggs, G. A. D. *Acc. Chem. Res.* **2005**, *38*, 901−909.
(5) Britz, D. A.; Khlobystov, A. N. *Chem. Soc. Rev.* **2006**, *35*, 637−659.
(6) Lu, T.; Goldfield, E. M.; Gray, S. K. *J. Chem. Phys. B* **2006**, *110*, 1742−1751.
(7) Lu, T.; Goldfield, E. M.; Gray, S. K. *J. Chem. Phys. B* **2003**, *107*, 12989−12995.
(8) Britz, D. A.; Khlobystov, A. N.; Porfyrakis, K.; Ardavan, A.; Briggs, G. A. D. *Chem. Commun.* **2005**, *15*, 37−39.
(9) Ulbricht, H.; Hertel, T. *J. Phys. Chem. B* **2003**, *107*, 14185−14190.
(10) Yoon, Y.; Berber, S.; Tomanek, D. *Phys. Rev. B* **2005**, *71*, art. no. 155406.
(11) Maniwa, Y.; Kataura, H.; Abe, M.; Fujiwara, A.; Fujiwara, R.; Kira, H.; Tou, H.; Suzuki, S.; Achiba, Y.; Nishibori, E.; Takata, M.; Sakata, M.; Suematsu, H. *J. Phys. Soc. Jpn.* **2003**, *72*, 45−48.
(12) Hirahara, K.; Bandow, S.; Suenaga, K.; Kata, H.; Okazaki, T.; Shinohara, H.; Iijima, S. *Phys. Rev.* **2001**, *64*, 115420/1−115420/5.
(13) Kataura, H.; Maniwa, Y.; Abe, M.; Fujiwara, A.; Kodama, T.; Kikuchi, K.; Imahori, H.; Misaki, Y.; Suzuki, S.; Achiba, Y. *Appl. Phys.* **2002**, *74*, 349−354.
(14) Smith, B. W.; Russo, R. M.; Chikkannanavar, S. B.; Luzzi, D. E. *J. Appl. Phys.* **2002**, *91*, 9333−9340.
(15) Moret, R.; Launois, P.; Persson, P. A.; Sundqvist, B. *Europhys. Lett.* **1997**, *40*, 55−60.

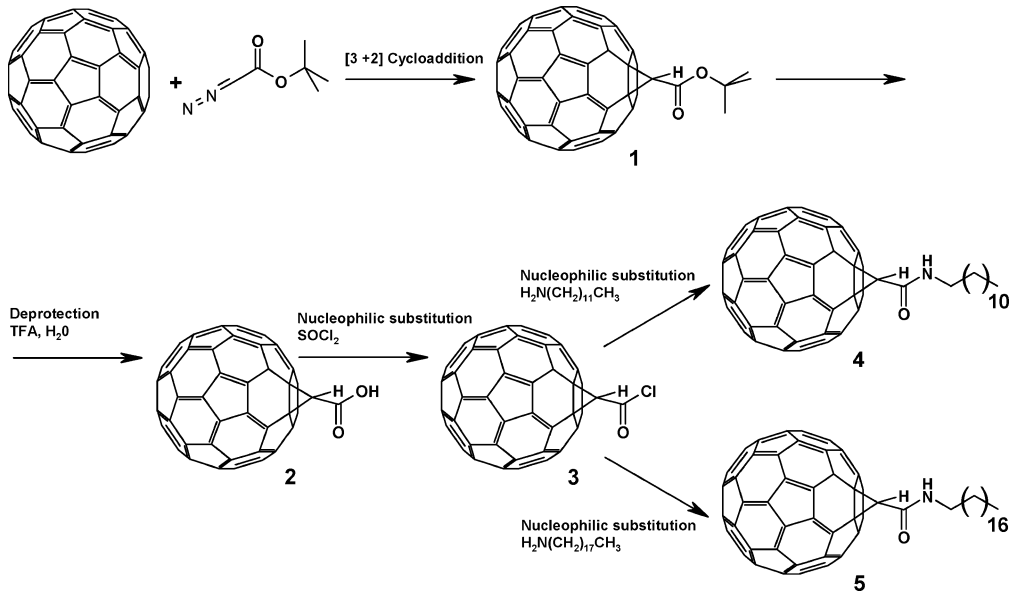

Figure 2. Scheme for preparation of **4** and **5**.

are mainly dictated by the van der Waals diameter of the fullerene carbon cages.

Since encapsulated molecules are often regarded as dopants locally perturbing and modulating the intrinsic electronic properties of carbon nanotubes[20−23] and viewed as potential carriers of quantum information,[24] the control of the intermolecular separations inside nanotubes is an important goal. For example, SWNT's band gap and the type, concentration, and mobility of change carriers have been demonstrated to be affected by the presence of the molecules. Provided that the number of molecules inserted in a nanotube is controlled, filling nanotubes with molecules could potentially be used as a facile method for fine-tuning the functional properties of SWNTs. Moreover, since carbon nanotubes have been proposed as miniature chemical reactors[8,25−27] the intermolecular separation is expected to be a crucial parameter for controlling chemical reactions inside nanotubes. However, to date, no practical approach for tuning the spacing between the molecules within quasi-1D arrays has been proposed. Potentially, there are two challenges in this area: the first is controlling the gross dopant density, which is important for tuning the nanotube's overall characteristics, such as conductivity, and the second is related to precise control of the spacing and geometric ordering of molecules, which is important for quantum properties of these structures. We have reasoned that introduction of chemical functionality on the fullerene cage may enable the control of the intermolecular spacing inside the nanotube beyond the van der Waals diameters of fullerene cages (Figure 1). In this study we explore the effect of alkyl groups on ordering and intermolecular separation of fullerenes inside the nanotube.

Results and Discussion

Fullerene Synthesis. Due to the availability of a wide variety of alkyl groups that are chemically and electronically relatively inert, we regarded them as ideal spacers for fullerenes inside nanotubes (Figure 1). Alkyl groups attached to fullerenes can create effective physical barriers between optically/magnetically active fullerene cages. Simple unbranched alkyl chains could provide essential steric bulk for achieving the increase in interfullerene separation, and being able to adopt numerous orientations, through rotations around the single carbon bonds, they provide more flexibility required for fullerenes to enter the nanotube than conformationally rigid functional groups (such as polyaromatic chains) of similar length. In this study we utilized carbon chains of two different lengths to allow comparison between chain length and resultant interfullerene separation to be made. The physical size and conformational flexibility of the linker between the alkyl chain and the fullerene cage are also important to consider, but these are expected to play a minor role as compared to the alkyl chain length. Ester and amide linkers were chosen as they are chemically inert under the nanotube filling conditions and are expected to be strong enough to resist the effects of the electron beam, when the resultant systems are imaged by HRTEM, for long enough to allow images to be acquired.[28]

The amide-linked fullerenes **4** and **5** were prepared according to the scheme outlined in Figure 2. Compound **2**[29] was converted to the amide derivatives of dodecylamine **4** and octadecylamine

(16) Hirahara, K.; Bandow, S.; Suenaga, K.; Kata, H.; Okazaki, T.; Shinohara, H.; Iijima, S. *Phys. Rev.* **2001**, *64*, 115420/1−115420/5.
(17) Maniwa, Y.; Kataura, H.; Abe, M.; Fujiwara, A.; Fujiwara, R.; Kira, H.; Tou, H.; Suzuki, S.; Achiba, Y.; Nishibori, E.; Takata, M.; Sakata, M.; Suematsu, H. *J. Phys. Soc. Jpn.* **2003**, *72*, 45−48.
(18) Okazaki, T.; Suenaga, K.; Hirahara, K.; Bandow, S.; Iijima, S.; Shinohara, H. *Physica* **2002**, *323*, 97−99.
(19) Suenaga, K.; Taniguchi, R.; Shimada, T.; Okazaki, T.; Shinohara, H.; Iijima, S. *Nano Lett.* **2003**, *3*, 1395−1398.
(20) Lee, J.; Kim, H.; Kahng, S.-J.; Kim, G.; Son, Y.-W.; Ihm, J.; Kato, H.; Wang, Z. W.; Okazaki, T.; Shinohara, H.; Kuk, Y. *Nature* **2002**, *415*, 1005−8.
(21) Hornbaker, D. J.; Kahng, S.-J.; Misra, S.; Smith, B. W.; Johnson, A. T.; Mele, E. J.; Luzzi, D. E.; Yazdani, A. *Science* **2002**, *295*, 828−831.
(22) Li, L.-J.; Khlobystov, A. N.; Wiltshire, J. G.; Briggs, G. A. D.; Nicholas, R. J. *Nat. Mater.* **2005**, *4*, 481−5.
(23) Basiuk, E. V.; Rybak-Akimova, E. V.; Basiuk, V. A.; Acosta-Najarro, D.; Saniger, J. M. *Nano Lett.* **2002**, *2*, 1249−1252.
(24) Benjamin, S. C.; Ardavan, A.; Briggs, G. A. D.; Britz, D. A.; Gunlycke, D.; Jefferson, J.; Jones, M. A. G.; Leigh, D. F.; Lovett, B. W.; Khlobystov, A. N.; Lyon, S. A.; Morton, J. J. L.; Porfyrakis, K.; Sambrook, M. R.; Tyryshkin, A. M. *J. Phys.: Condens. Matter*. **2006**, *18*, 867−883.
(25) Costa, P. M. F. J.; Sloan, J.; Rutherford, T.; Green, M. L. H. *Chem. Mater.* **2005**, *17* (26), 6579−6582.
(26) Halls, M. D.; Schlegel, H. B. *J. Phys. Chem.* **2002**, *106*, 1921.
(27) Halls, M. D.; Raghavachari, K. *Nano Lett.* **2005**, *5* (10), 1861−1866.
(28) Although it is difficult to assess the extent of the e-beam effect on alkyl-functionalized fullerenes, it has been minimized as much as possible by reducing the accelerating voltage in TEM to 100 kV and the exposure time to 2−3 s.

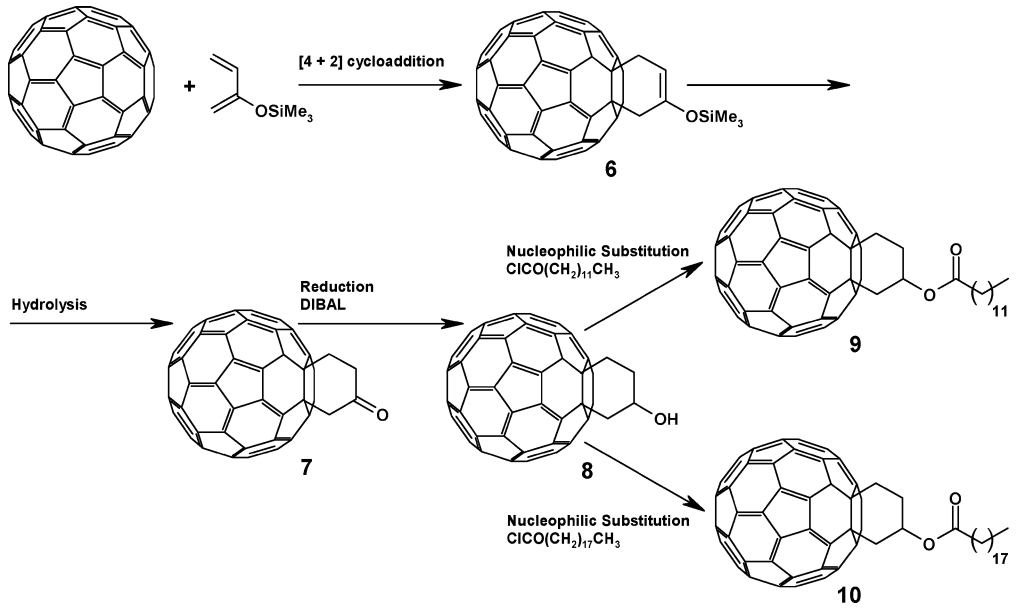

Figure 3. Scheme for preparation of **9** and **10**.

5 via 1,2-(3′-chloroformylcyclopropano)[60]fullerene, **3**, in high yields.[30,31] The ^{1}H NMR spectrum of **4** (Supporting Information) provided the characteristic peaks at 6.4 ppm (CH_2 b), the multiplet at 3.6 ppm (CH_2 c), the singlet at 4.7 ppm (CH d, the cyclopropane hydrogen), and the multiplets in the range 1.5−0.9 assigned to the remaining protons on the alkyl chain. The ^{13}C NMR spectrum provided peaks at 72 ppm (assigned to the cyclopropane atom C_d), 42 ppm (C_b of the alkyl chain), 41 ppm (C_c of the alkyl chain), peaks in the range 133−160 ppm (assigned to the 12 predicted environments of the fullerene carbon atoms and C_a of the amide group), and finally the peaks in the range 14−33 ppm (assigned to the remaining alkyl-chain carbons). The IR spectrum showed a carbonyl stretch at 1640 cm^{-1}, supporting the above data for the formation of an amide functional group in **4**. The second amine chosen was octadecylamine. This would provide a longer chain than **4** and would make for an interesting comparison. Octadecylamine was added to 1,2-(3′-chloroformylcyclopropano)[60]fullerene to produce the 1,2-(3′-octadecanaminoformylcyclopropano)[60]fullerene, **5,** under conditions identical to those for the synthesis of **4**. The ^{1}H and ^{13}C NMR spectra of **5** (Supporting Information) includes similar characteristic peaks to the analogous spectrum for **4**.

The alternative, ester-linked, functionalized fullerenes **9** and **10** were prepared according to the scheme outlined in Figure 3. The cyclohexane linker is expected to be more stable than the strained cyclopropane ring in **4** and **5** and thus should provide a more robust attachment of the alkyl groups to fullerene cages, stable at higher temperatures and under HRTEM imaging conditions.

The two acyl chlorides reacted with the hydroxyl group of the intermediate **8**[32] were tridecanoyl chloride and nonadecanoyl chloride, as they are readily available and are long enough to provide enough steric bulk for a noticeable separation between fullerenes without being too long to inhibit the fullerene encapsulation process. The alkyl chains are the same length as the analogous amide fullerenes **4** and **5**, allowing direct comparison between the two types of functionalized fullerenes. The products **9** and **10** were characterized by ^{1}H and ^{13}C NMR and matrix-assisted laser desorption ionization time-of-flight mass spectrometry (MALDI-TOF MS) confirming the structure of the molecules. The ^{1}H NMR data provided the characteristic peak at 6.14 ppm for **9** (6.12 ppm for **10**) assigned to the proton attached to the carbon linking the six-membered ring to the ester chain, peaks in the region 3.69−2.78 ppm for **9** (3.72−2.75 ppm for **10**) corresponding to the cyclohexane ring protons, and a peak at 3.72 ppm assigned to the protons of the CH_2 group next to the ester linker.

Encapsulation of Functionalized Fullerenes in Carbon Nanotubes. The functionalized fullerene molecules **4**, **5**, **9**, and **10** were inserted into SWNTs by mixing a 3-fold excess of the solid fullerene with air-annealed, opened SWNTs (major diameters = 13.6 and 14.9 Å)[33] in supercritical CO_2 ($scCO_2$) following the previously reported procedure.[3] Nonencapsulated fullerene molecules were recovered by extensive washing with CS_2 and the remaining material was examined by high-resolution transmission electron microscopy (HRTEM). The imaging conditions were set to minimize knock-on damage commonly occurring in fullerene structures under exposure to the electron beam. The accelerating voltage was set at 100 kV, the beam current on the specimen was reduced to minimum, and exposure times were 1−2 s to minimize the damage. Imaging of C_{60}@SWNT under these conditions showed no structural changes in peapods over 10 min.

Approximately 10% of SWNTs were found to be filled with fullerene molecules (for all samples). These filling yields were considerably lower than in the previously reported case of C_{60}@SWNT (>70%). The lower yields for alkyl-functionalized fullerenes (compounds **4**, **5**, **9**, and **10**) can be explained by considering the complex shape and the high aspect ratio of the

(29) Isaacs, L.; Wehrsig, A.; Diederich, F. *Helv. Chim. Acta* **1993**, *76*, 1231−1250.
(30) Tada, T.; Ishida, Y.; Saigo, K. *J. Org. Chem.* **2006**, *71*, 1633−1639.
(31) Sun, Y.-P.; Lawson, G. E.; Riggs, J. E.; Ma, B.; Wang, N.; Moton, D. K. *J. Phys. Chem.* **1998**, *102*, 5520−5528.
(32) An, Y.; Chen, C. B.; Anderson, J. L.; Sigman, D. S.; Foote, C. S.; Rubin, Y. *Tetrahedron* **1996**, *52*, 5179−5189.
(33) Khlobystov, A. N.; Scipioni, R.; Nguyen-Manh, D.; Britz, D. A.; Pettifor, D. G.; Briggs, G. A. D.; Lyapin, S. G.; Ardavan, A.; Nicholas, R. J. *Appl. Phys. Lett.* **2004**, *84*, 792.

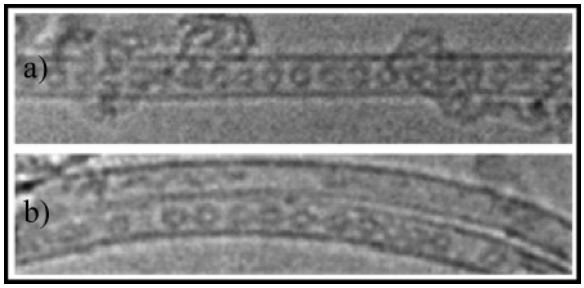

Figure 4. HRTEM of (a) C_{60}@SWNT and (b) $C_{61}(COOEt)_2$@SWNT.

$C_{60}X$ molecules (where X is the attached functional group) when compared with the simple spherical shape of C_{60}. The alkyl tail may inhibit the entry of the carbon cage into the nanotube as the long tail will preclude the fullerene cage rolling on the nanotube surface and down the tube once the molecules are inside. The alkyl chain also increases the solubilization of the molecules with $scCO_2$, which may affect the insertion rate.

In HRTEM images the C_{60} molecules appear as circles with diameters of ~7.0 Å sandwiched between two parallel lines corresponding to the nanotube (Figure 4), which is the expected form of the projected three-dimensional C_{60}@SWNT structures (Figure 1). Images of individual peapods consistently show circles within lines with no overlapping of the two, proving that the C_{60} molecules are encapsulated within the nanotubes and not adhered to the outside walls.

Pure C_{60} (Figure 4a) appears as a perfect circle, whereas the functionalized fullerenes, such as cyclopropanated $C_{61}(COOEt)_2$ (Figure 4b), appear elongated or oval in shape. The elongation in shape can be explained by a loss in the degree of symmetry after functionalization and also by the effect of the electron beam being more pronounced for the thermodynamically less stable functionalized fullerenes.

The HRTEM micrographs in Figure 5 show typical geometries of alkyl-functionalized fullerenes **4**, **5**, **9**, and **10** encapsulated in SWNTs (see Supporting Information for more examples).

Interfullerene spacing analysis was conducted on images of these four types of fullerenes. The method used for this study involved mapping circles of diameters corresponding to the diameter of the fullerene cage C_{60} (~7 Å) onto TEM images of $C_{60}X$@SWNT structures and then measuring the distances between the centers of neighboring circles (for details see Supporting Information). Although the functionalized fullerene cages appear as distorted circles in HRTEM, this does not affect the measurement of interfullerene distances as these are measured from the center of one fullerene cage to the center of the neighboring fullerene cage. The encapsulation of C_{60} in SWNT was carried out under the same conditions as a control; the observed spacing of 9.80 Å was included for comparison. Alkyl-chain-functionalized fullerenes exhibit a much greater spread of intermolecular spacings in carbon nanotubes than C_{60}, which results in no observable long-range order in $C_{60}X$@SWNT structures as compared with almost perfectly periodic C_{60}@SWNTs (Figure 4a). The lack of periodicity in $C_{60}X$@SWNT can be explained by conformational flexibility of the alkyl group attached to fullerenes, which can adopt different folding arrangements inside the nanotube (Figure 6).

However, the interfullerene spacings of **4** and **9** encapsulated in SWNTs both show a frequently occurring common spacing

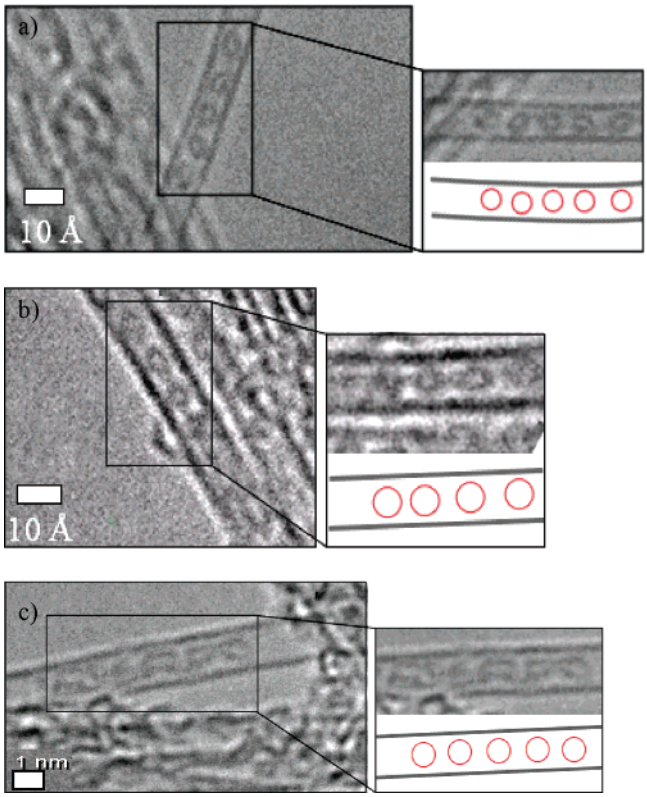

Figure 5. HRTEM images of (a, b) **4**@SWNT and (c) **5**@SWNT, with peapod system and diagrammatic representations of the fullerene positions to the right.

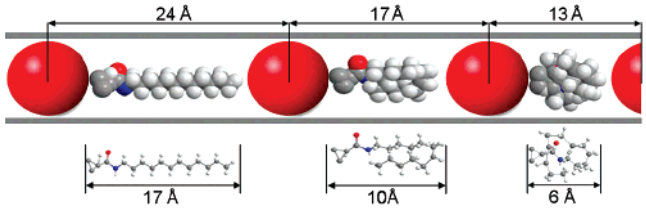

Figure 6. Schematic representation of folding variations of the alkyl chain ($C_{12}H_{25}$) in $C_{60}X$@SWNT structures (where $C_{60}X$ = **4** or **9**).

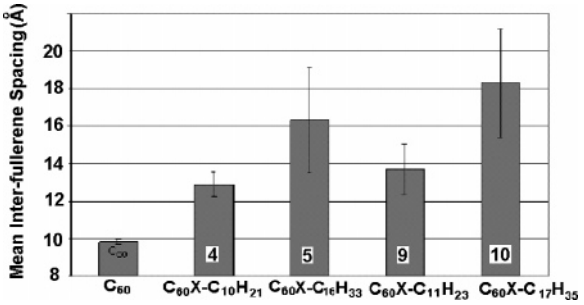

Figure 7. Mean interfullerene spacing for C_{60}@SWNT, **4**@SWNT, **5**@SWNT, **9**@SWNT, and **10**@SWNT peapod structures.

of approximately 13 Å, which presumably corresponds to the most compact conformation of the alkyl chain (see Figure 6) and relates to the smallest volume the alkyl tail $C_{12}H_{25}$ can occupy between fullerene cages.

Despite the disordered arrangement of alkyl-functionalized fullerenes, it was possible to calculate the mean interfullerene separations for the fullerene derivatives (Figure 7). The average spacing in all $C_{60}X$@SWNT structures is significantly higher than that observed for C_{60}@SWNT (9.80 Å) assembled and

examined under the same conditions. The observed increase of the intermolecular separation can thus be attributed to the presence of alkyl chains attached to the fullerene cages. The observed interfullerene separations for the two shorter-tailed fullerenes **4** and **9** (alkyl group = $C_{12}H_{25}$, full extended length = 17 Å) are systematically shorter than the separations of the two longer-chained fullerenes **5** and **10** (alkyl group = $C_{18}H_{37}$, full extended length = 26 Å). This result was predicted and is attributed to the greater number of atoms and subsequently larger volume of the respective carbon chains. Since the nanotube diameter distribution in these samples is in a narrow range (major diameters 13.6 and 14.9 Å), the slight diameter variation from one nanotube to another is unlikely to have a measurable effect on the fullerene positions. The fullerene positions could be affected if the nanotube diameters would vary in a wider range (11−25 Å), as demonstrated earlier for double-walled and multiwalled carbon nanotubes.[34]

Conclusions

We have synthesized a range of fullerenes functionalized with sterically bulky alkyl chains in order to study the impact of the functional groups on the intermolecular spacing in nanotubes.[35] It has been demonstrated that the presence of alkyl groups attached to fullerene cages significantly increases the mean intermolecular separations but disrupts the periodicity of the fullerene arrays, yielding disordered chains of $C_{60}X$ molecules. Comparison of alkyl groups of different length has proved that bulkier spacers provide larger interfullerene separations. This indicates that this approach is in principle viable for controlling the position and the density of molecules in SWNTs, and therefore can potentially be utilized for tuning the electronic properties of these hybrid systems. However, spacers conformationally more rigid than alkyl chains are expected to be more suitable for arranging ordered molecular arrays inside nanotubes.

Experimental Section

Arc-discharge-produced SWNTs (Aldrich) were used for the experiments. Raw nanotubes were purified by annealing in air at 420 °C for 20 min to remove amorphous carbon and to open their termini. C_{60} (99.5%) was purchased from SES Research. All other reagents and solvents were purchased from Aldrich and were used without further purification. Elemental analyses (C, H, N) were performed by the University of Nottingham School of Chemistry Microanalytical Service on a Perkin-Elmer 240B instrument. Infrared spectra were measured as either KBr discs or in solution on a Nicolet Avatar 380 FT-IR spectrometer over the range 400−4000 cm^{-1}. ^1H and ^{13}C NMR spectra were obtained on a Bruker DPX 300 spectrometer. Mass spectrometry was carried out on a FAB-LSIMS spectrometer and a MALDI-TOF spectrometer at the EPSRC National Mass Spectrometry Service Centre in Swansea.

HRTEM analysis was performed on a JEOL-JEM 4000EX LaB_6 microscope with an information limit of 0.12 nm. The imaging conditions were carefully tuned by lowering the accelerating voltage of the microscope to 100 kV and reducing the beam current density to a minimum. Nanotube samples (2−3 mg) were dispersed in 2 mL of methanol by use of an ultrasonic bath and deposited onto lacey carbon film-coated TEM copper grids. The filling rates were determined by taking micrographs of 100 nm^2 areas from different regions of the specimen, estimating the proportion of filled nanotubes for each area, and averaging the filling factors over 50−70 areas.

Fullerene Synthesis. Compounds **1**−**3** were prepared by methods reported previously in the literature.[24]

Procedure for 1,2-(3′-Dodecanaminoformylcyclopropano)^{60}-fullerene, 4. A solution of dodecylamine (116.77 mg, 0.0063 mmol) dissolved in dry toluene (5 mL) was added dropwise with stirring to a refluxing solution of **3** (4.90 mg, 0.0061 mmol) dissolved in dry toluene (35 mL). The resulting orange solution was refluxed at 110 °C under N_2 for 4 h. The resulting red solution was cooled to room temperature and the solvent was removed under reduced pressure. The resulting brown solid was dissolved in carbon disulfide (2 mL), and column chromatography [silica, toluene/ethanol (99:1)] afforded the crude product (6.30 mg, 0.0067 mmol) as a brown solid. Further column chromatography [silica, toluene/ethyl acetate (9:1)] afforded the product, 1,2-(3′-dodecanaminoformylcyclopropano)^{60}fullerene **4** (4.10 mg, 0.0043 mmol, 69%), as a brown solid. ^1H NMR {300 MHz, $CDCl_3$, 300 K} δ_H 6.39 (s, 1H, N*H*), 4.70 (s, 1H, C*H*CONR), 3.58 (m, 2H, CONHCH_2R), 1.8−0.8 [br m, 23H, alkyl chain (CH_2)$_{10}$CH_3] ppm. ^{13}C NMR {300 MHz, $CDCl_3$, 300 K} δ_C 167.3, 145.7,145.3, 145.2, 144.8, 144.7, 144.5, 143.3, 143.1, 142.0, 141.3, 140.0, 136.3, 71.9, 42.2, 40.7, 32.3, 30.1, 30.0, 29.8, 29.8, 27.5, 23.2, 14.5 ppm. MALDI-MS 945.2 *m*/*z* [M]$^-$. IR (KBr disk) 3390.72 m, 3192.74 m, 2822.50 m, 2306.12 w, 1669.13 s, 1385.07 m, 1169.87 m, 885.81 w cm^{-1}.

Procedure for Preparing 1,2-(3′-Octadecanaminoformylcyclopropano)^{60}fullerene, 5. A solution of octadecylamine (121.30 mg, 0.45 mmol) dissolved in dry toluene (5 mL) was added dropwise with stirring to a refluxing solution of **3** (5.10 mg, 0.0064 mmol) dissolved in dry toluene (35 mL). The resultant orange solution was refluxed at 110 °C under N_2 for 4 h. The resulting red solution was cooled to room temperature and the solvent was removed under reduced pressure. The resultant brown solid was dissolved in carbon disulfide (2 mL), and column chromatography [silica, toluene/ethanol (99:1)] afforded the crude product (6.70 mg, 0.0065 mmol) as a brown solid. Further column chromatography [silica, toluene/ethyl acetate (9:1)] afforded the product, 1,2-(3′-octdecanaminoformylcyclopropano)^{60}fullerene, **5** (4.80 mg, 0.0047 mmol, 73%), as a brown solid. ^1H NMR {300 MHz, $CDCl_3$, 300 K} δ_H 6.40 (s, 1H, N*H*), 4.69 (s, 1H, C*H*CONR), 3.57 (m, 2H, CONHCH_2R), 1.7−0.7 [br m, 35H, alkyl chain (CH_2)$_{16}$CH_3] ppm. ^{13}C NMR {300 MHz, $CDCl_3$, 300 K} δ_C 168.2, 145.6, 145.3, 145.1, 145.0, 144.6, 143.3, 143.2, 132.9, 131.3, 129.2, 68.6, 39.1, 32.3, 30.8, 30.1, 29.8, 29.3, 24.1, 23.4, 23.1, 14.5, 14.5, 11.4 ppm. FAB-MS 1030.3 *m*/*z* [M]$^+$. MALDI-MS 1030.3 *m*/*z* [M]$^-$. IR (KBr disk) 3287.43 w, 2960.33 s, 2874.24 s, 2805.38 m, 1672.35 s, 1453.93 m, 1385.07 w, 1126.83 m cm^{-1}.

Preparation of Ester-Linked Alkylated Fullerenes 9 and 10. The protected diene 2-trimethylsilyloxy-1,3-butadiene, **6**, and fullerene compounds **7** and **8** were synthesized according to the literature (see Supporting Information for full method).[27]

Procedure for Preparing 1,2-[4′-(Tridecyl ester)cyclohexano]^{60}-fullerene, 9. A solution of **8** (3.06 mg, 0.0039 mmol) dissolved in dry toluene (30 mL) was refluxed at 110 °C under N_2 for 10 min, then a solution of tridecanoyl chloride (112.20 mg, 0.52 mmol) in dry toluene (2 mL) was added dropwise with stirring, and the resultant orange solution was refluxed for 4 h. The solution was cooled and the solvent was removed under reduced pressure to afford a brown solid crude product, which was dissolved in carbon disulfide (2 mL). Column chromatography (silica, toluene) followed by further column chromatography [silica, chloroform/ethanol (99:1)] afforded the pure product, 1,2-[4′-(tridecyl ester)cyclohexano]^{60}fullerene, **9** (3.12 mg, 0.0032 mmol, 81%) as a brown solid. ^1H NMR {300 MHz, $CDCl_3$, 300 K} δ_H 6.14 (m, 1H, aromatic H), 3.72 (t, $^3J_{H-H}$ = 7.1 Hz, 2H, COCH_2), 3.69 (m, 2H, aromatic H), 3.49 (m, 2H, aromatic H), 3.32 (m, 1H, aromatic H), 2.78 (m, 1H, aromatic H), 2.50 (t, $^3J_{H-H}$ = 7.1 Hz, 2H, COCH$_2$CH_2), 1.7−0.8 [br m, 21H, alkyl chain (CH_2)$_9$CH_3] ppm. ^{13}C NMR {300 MHz, $CDCl_3$, 300 K} δ_C 172.4, 147.3, 147.1, 146.9, 144.7,

(34) Khlobystov, A. N.; Britz, D. A.; Ardavan, A.; Briggs, G. A. D. *Phys. Rev. Lett.* **2004**, *92*, art. no. 245507.
(35) While this paper was under consideration, a study on alkyl-chain-functionalized *o*-carborane molecules in carbon nanotubes has been published online: Koshino, M.; Tanaka, T.; Solin, N.; Suenaga, K.; Isobe, H.; Nakamura, E. *Science* **2007**, *316*, 853.

144.6 144.3, 141.8, 140.5, 139.9, 72.4, 33.9, 32.5, 31.4, 31.3, 30.1, 30.0, 29.8, 29.7, 29.5, 27.1, 25.4, 23.1, 21.1, 21.0, 14.1 ppm. MALDI-MS 988.3 *m*/*z* $[M]^-$. IR (KBr disk) 3041.18 m, 2965.85 s, 2932.36 s, 2882.14 s, 2672.88 m, 1710.27 s, 1467.53 m, 1417.30 w, 1300.12 m, 948.55 w cm^{-1}.

Procedure for Preparing 1,2-[4′-(Nonadecyl ester)cyclohexano][60]-fullerene, 10. A solution of **8** (4.21 mg, 0.0053 mmol) dissolved in dry toluene (30 mL) was refluxed at 110 °C under N_2 for 10 min, then a solution of tridecanoyl chloride (106.40 mg, 0.36 mmol) in dry toluene (2 mL) was added dropwise with stirring, and the resultant orange solution was refluxed for 4 h. The solution was cooled and the solvent was removed under reduced pressure to afford a brown solid crude product, which was dissolved in carbon disulfide (2 mL). Column chromatography (silica, toluene) followed by further column chromatography [silica, chloroform/ethanol (99:1)] afforded the pure product, 1,2-[4′-(nonadecyl ester)cyclohexano][60]fullerene, **10** (4.59 mg, 0.0043 mmol, 81%) as a brown solid. ^{1}H NMR {300 MHz, $CDCl_3$, 300 K} δ_H 6.12 (m, 1H, aromatic H), 3.72 (t, $^3J_{H-H} = 7.3$ Hz, 2H, $COCH_2$), 3.70 (m, 2H, aromatic H), 3.41 (m, 2H, aromatic H), 3.35 (m, 1H, aromatic H), 2.75 (m, 1H, aromatic H), 2.47 (t, $^3J_{H-H} = 7.3$ Hz, 2H, $COCH_2CH_2R$), 1.8−0.7 [br m, 33H, alkyl chain $(CH_2)_9CH_3$] ppm. ^{13}C NMR {300 MHz, $CDCl_3$, 300 K} δ_C 171.9, 145.8, 145.4, 145.1, 144.8, 141.9, 141.3, 140.7, 140.6, 139.9, 136.8, 73.2, 33.7, 32.4, 31.2, 31.1, 30.0, 29.9, 29.8, 29.6, 29.5, 28.6, 25.2, 21.0, 20.8, 13.9 ppm. FAB-MS 1073.3 *m*/*z* $[M]^+$. MALDI-MS 1073.3 *m*/*z* $[M]^-$. IR (KBr disk) 2949.34 m, 2917.56 s, 2849.46 s, 1705.36 s, 1469.27 m, 1432.95 m, 1410.25 m, 942.62 w cm^{-1}.

Nanotube Filling in Supercritical Fluids. Purified nanotubes were annealed in air at 420 °C for 30 min shortly before mixing with fullerenes. Approximately a 3-fold excess of fullerene was dissolved in a minimum amount of carbon disulfide, the resultant solution was deposited onto the SWNTs, and the solvent was evaporated at room temperature. Typically 5 mg of the fullerene/nanotubes mixture was placed in a glass tube and the tube was filled with CO_2 at 150 bar. In pressure cycling experiments, the pressure in the tube was decreased from 150 to 100 bar over approximately 12 h at 50 °C, and then the tube was pressurized again to 150 bar and the cycle repeated every 24 h. After several days of exposure to the supercritical fluid at 50 °C, the mixture was washed with carbon disulfide (10 mL) in order to remove the excess nonencapsulated fullerenes.

Acknowledgment. The $scCO_2$ filling experiments were carried out with technical assistance from Professor Martyn Poliakoff and Dr. Paul Hamley at the University of Nottingham. This work was supported by The University of Nottingham, the Engineering and Physical Sciences Research Council (EPSRC, EP/C545273/1 and GR/S15808/01), the European Science Foundation (ESF), and the Royal Society.

Supporting Information Available: Experimental data, HR-TEM images, and full statistical analysis of peapod systems. This material is free of charge via the Internet at http://pubs.acs.org.

JA071803Q